Weiner, S. J., Kollman, P. A., Case, D. A., Singh, U. C., Ghio, C., Alagona, G., Profeta, S., Jr., & Weiner, P. K. (1984) *J. Am. Chem. Soc. 106*, 765–784.
Wherland, S., & Gray, H. B. (1977) in *Biological Aspects of Inorganic Chemistry* (Addison, A. W., Cullen, W. R., Dolphin, D. & James, B. R., Eds.) pp 289–368, Wiley, New York.
Yagi, T. (1970) *J. Biochem. (Tokyo) 68*, 649–657.
Yagi, T., Inokuchi, H., & Kimura, K. (1983) *Acc. Chem. Res. 16*, 2–7.

Cytochrome *c* and c_2 Binding Dynamics and Electron Transfer with Photosynthetic Reaction Center Protein and Other Integral Membrane Redox Proteins†

C. C. Moser* and P. Leslie Dutton
Department of Biochemistry and Biophysics, University of Pennsylvania, Philadelphia, Pennsylvania 19104
Received July 22, 1987; Revised Manuscript Received December 2, 1987

ABSTRACT: To further the understanding of the details of *c*-type cytochrome action as a redox carrier between major electron-transfer proteins, the single-turnover kinetics time course of cytochrome *c* and cytochrome c_2 oxidation by flash-activated photosynthetic reaction center (purified from the bacterium *Rhodobacter sphaeroides*) has been examined under a wide variety of conditions of concentration, ionic strength, and viscosity with reaction center present in detergent dispersion and phosphatidylcholine proteoliposomes. We find that the three-state model proposed by Overfield and Wraight [Overfield, R. E., & Wraight, C. A. (1980) *Biochemistry 19*, 3322–3327] is generally sufficient to model the kinetics time course; many similarities are found with the cytochrome *c*–cytochrome *c* oxidase interaction in mitochondria. Further, we find the following: (1) Significant "product inhibition" by oxidized cytochrome *c* (c_2) bound to the reaction center is apparent. (2) The viscosity sensitivity of the electron transfer into the reaction center from bound cytochrome *c* (c_2) suggests a physical interpretation of the distal state. (3) The exchange dynamics of oxidized and reduced cytochrome *c* (c_2) are similar regardless of the state of activation of the reaction center. (4) Preferential binding of the oxidized form of cytochrome *c* is revealed upon reconstitution of the reaction center into neutral lipid vesicles, permitting an independent confirmation of the binding suggested by the kinetics. (5) Flash-activated electron-transfer kinetics in reaction center hybrid protein systems have shown that diffusion and competitive binding characterize the behavior of cytochrome *c* as a redox carrier between the reaction center protein and either the cytochrome bc_1 complex or the cytochrome *c* oxidase.

Cytochromes of the *c* type have been intensively studied for many years. Since many are small, water soluble, and crystallizable, they have provided a convenient vehicle for study of a wide variety of questions of cytochrome structure–function using almost all biochemical and physical techniques. In physiological terms, their role is well established (Dutton, 1986). In prokaryotic and eukaryotic respiratory systems, a cytochrome (cyt)[1] *c* operates to shuttle electrons between the much larger integral membrane redox proteins, ubiquinol–cyt-*c* oxidoreductase (cyt bc_1 complex) and cytochrome *c* oxidase. In photosynthetic bacteria, they act similarly between analogous ubiquinol–cyt-c_2 oxidoreductase and the photochemical reaction center (RC) protein. In all these systems, the structural arrangement is the same: the cyt *c* is located in the aqueous periplasmic space outside the intracytoplasmic membrane and inside the outer membrane or cell wall. The subunits of the membrane redox proteins containing immediate electron-donating or -accepting redox components for cyt *c* are exposed to the periplasm; cyt *c* appears to diffuse between these reaction sites along the membrane–aqueous interface and through the aqueous solution (Hochman et al., 1985; Vanderkooi et al., 1985; Ferguson-Miller et al., 1986). At another level, investigations into the structure and dynamics of cyt *c* complexation with the membrane protein sites where electron transfer occurs have been fewer; nevertheless, useful models built upon early observations interpreted as multiple binding states of cyt *c* with cyt *c* oxidase (Ferguson-Miller et al., 1976) and reaction center proteins (Dutton et al., 1975; Dutton & Prince, 1978) have been presented.

A unique route to the understanding of the details of cyt *c* action as a redox carrier between major electron-transfer proteins is offered by photosynthetic bacteria, where the opportunity to initiate electron transfer by light provides far-reaching experimental benefits. The delivery of a brief flash of light that turns over the RC just once permits the electron-transfer reactions such as cyt *c* oxidation to be studied without the complications attendant with steady-state analysis; elementary first- and second-order reactions can be monitored as they progress and transient states are revealed. The approach has the potential to expose binding properties, stable and unstable reaction states, and also functional details that would be difficult or perhaps impossible to uncover with conventional forms of activation.

The first application of this approach with isolated RC preparations was by Ke et al. (1970). They used early, high molecular weight RC preparations in the detergent Triton and

† Supported by U.S. Public Health Service Grant GM 27309.
* Address correspondence to this author at the Department of Biochemistry and Biophysics, B501 Richards Building, University of Pennsylvania, Philadelphia, PA 19104.

[1] Abbreviations: $[BChl]_2$ and $[BChl]_2^+$, normal and oxidized bacteriochlorophyll dimer, respectively; cyt, cytochrome; cyt bc_1 complex, ubiquinol–cytochrome-*c* (c_2) oxidoreductase; EDTA, ethylenediaminetetraacetic acid; K_D, dissociation constant; LDAO, lauryldimethylamine oxide; *Rb.*, *Rhodobacter*; RC, reaction center; Tris-HCl, tris(hydroxymethyl)aminomethane hydrochloride; SDS, sodium dodecyl sulfate.

0006-2960/88/0427-2450$01.50/0

described 24 weak cyt *c* binding sites. Subsequently, as the minimal RC preparation was defined (Feher & Okamura, 1978), the number of binding sites also diminished. The most common values are 1 (Rosen et al., 1979) and 2 (Dutton & Prince, 1978; Overfield et al., 1979; Pachence et al., 1978, 1979a). The cyt *c* binding affinity, as given by the dissociation constant (K_D) measured in comparable ionic media (typically 10 mM Tris-HCl), has been found to be 0.4 μM in a 0.1% Triton preparation (Rosen et al., 1979), while a K_D range of 0.3–10 μM has been found for RC prepared in lauryldimethylamine oxide (LDAO) (Rosen et al., 1979; Overfield & Wraight, 1980a; Rickle & Cusanovich, 1979); increasing the detergent concentration to 2% weakens the binding considerably for both *Rhodobacter sphaeroides* and *Rhodospirillum rubrum* RC (Prince et al., 1974; Rickle & Cusanovich, 1979). In phospholipid bilayer RC preparations, the RC has been shown to orient with up to 90% vectorial asymmetry with the $[BChl]_2$ of the RC disposed to oxidize cyt *c* added to the outside of the vesicle (Pachence et al., 1978, 1979a,b). In these systems, cyt *c* binding and subsequent electron-transfer kinetics can be significantly influenced by competitive binding of cyt *c* to lipids of negative charge (Overfield & Wraight, 1980b; Packham et al., 1987); howevr, if the RC is reconstituted in neutral lipids, this complication is eliminated (Overfield & Wraight, 1980a).

Use of low ionic strengths and low or zero detergent concentrations to promote the well-known electrostatic association of cyt *c* with its electron donor/acceptor proteins such as cyt *c* oxidase or the RC has permitted some characterization of the reaction of the bound states of *c* cytochrome. In addition to multiple binding sites suggested by steady-state electron-transfer studies, both the RC and the cytochrome oxidase systems display kinetically distinct phases of oxidation (Ferguson-Miller et al., 1976; Dutton et al., 1975). In the case of the cyt *c*–RC system, a three-state model has been described (Overfield & Wraight, 1980a) to account for the multiphasic cyt *c* oxidation kinetics that had been observed in vitro and in vivo (Dutton et al., 1975). These states have been labeled for convenience as "off" for the unbound cyt *c*, "distal" for the bound cyt *c* that transfers its electron on the slower time scale, and "proximal" for the rapidly reacting bound cyt *c*.

The work presented here defines the dynamic properties of the interaction of cyt *c* and c_2 with the RC in detergent dispersions or when reconstituted in neutral phospholipid bilayers. It expands the analysis of electron transfer from cyt *c* to the RC to fit the entire kinetics time course successfully to the three functional state model under a wide variety of conditions. In particular, we describe the viscosity sensitivity of the bound state kinetics which, in combination with orientational and electrostatic observations (Tiede, 1987; Koppenol & Margoliash, 1982), suggest a physical interpretation of the distal state. We also describe a significant product inhibition that can occur even on a single-turnover flash. The recognition of this form of inhibition may help to reconcile our observations of RC light activation independent cyt *c* exchange dynamics with earlier interpretations (Overfield & Wraight, 1986). We extend the analysis to include cyt c_2, showing the validity of the general model with the appropriate adjustment of individual rates. In addition, the role of cyt *c* binding with other electron-transfer proteins is recognized in the diffusional kinetics of cyt *c* between RC and cyt *c* oxidase or cyt bc_1 complex in hybrid protein systems.

Materials and Methods

LDAO-solubilized RC protein was prepared from the photosynthetic bacterium *Rb. sphaeroides* blue-green mutant R-26 essentially as described (Clayton & Wang, 1971) with the modification that the chromatophores were initially extracted with 1.2% (vs 0.6%) LDAO. The RC preparation was dialyzed against 10 mM Tris, pH 8.0, overnight at 5 °C to remove excess salt and detergent that influences kinetics. SDS gel electrophoresis reveals only the three bands associated with the L, M, and H polypeptide subunits of the RC; 280- to 800-nm absorbance ratios were typically 1.25.

For an alternative detergent preparation, octyl glucoside solubilized RC protein was prepared by loading LDAO-solubilized RC on a DEAE-cellulose anion-exchange column and washing at room temperature with 4 L of 10 mM Tris, pH 8.0, at which point RC would not elute even with 1 M NaCl. A chaser of 50 mL of 30 mM octyl glucoside/10 mM Tris, pH 8.0, was slowly passed through the column before elution with 60 mM octyl glucoside, 500 mM NaCl, and 10 mM Tris, pH 8.0. Dialysis against 45 mM octyl glucoside/10 mM Tris, pH 8.0, overnight at 5 °C removed excess salt. Detergent-solubilized RC protein was stored in liquid nitrogen.

To study RC protein in a lipidic environment, LDAO-solubilized RC protein was incorporated into egg phosphatidylcholine vesicles through reductive destruction of LDAO, sonication, and dialysis as described (Pachence et al., 1979b). Alternatively, octyl glucoside solubilized RC protein was incorporated into vesicles, without the need for the reduction process, through detergent dialysis in the following way. An ethanolic solution of egg phosphatidylcholine was dried down under argon, RC protein solubilized in 45 mM octyl glucoside was added to lipid at a molar ratio (RC to lipid) of 0.01, and the solution was sonicated for 2 min before overnight dialysis against 4 L of 10 mM Tris, pH 8.0 at 5 °C. The sample was pelleted by ultracentrifugation and resuspended in 10 mM Tris, pH 8.0, buffer.

Equine cyt *c* (Sigma type VI) was dialyzed to remove salt or purified with a CM-cellulose cation-exchange column (Whatman), washed with 50 mM NaCl/10 mM Tris, pH 8.0, and eluted with 300 mM NaCl, followed by dialysis against 10 mM Tris, pH 8.0, for 1 h at room temperature to remove excess salt. Cyt c_2 was isolated and purified from *Rb. sphaeroides* as described (Bartsch, 1971).

The ubiquinol–cyt-*c* oxidoreductase (cyt bc_1 complex) and the cyt *c* oxidase were prepared from beef heart mitochondria according to the methods of Hatefi and Stiggal (1978) and Yonetani (1967), respectively. Final solubilization of both proteins was in cholate detergent. These proteins in "hybrid" combination with RC were prepared in detergent-solubilized solution as described (Moser et al., 1986).

Kinetic measurements were performed on an unchopped double-beam kinetic spectrophotometer (Johnson Research Foundation). The sample was kept under an argon atmosphere in an anaerobic glass cuvette fitted with a calomet–platinum electrode pair and a magnetic stir bar. Redox mediator dyes ferro-EDTA, diaminodurine (tetramethyl-1,4-benzoquinone), pyocyanine (1-hydroxy-5-methylphenazinium hydroxide), and 2-hydroxy-1,4-naphthoquinone were kept to minimal concentrations needed to establish effective redox potential readings on a tens of seconds time scale and to prevent interference with millisecond electron-transfer kinetics (Dutton, 1978; Moser et al., 1986). Excitation of the RC protein was accomplished with a xenon flash of approximately 8-μs duration (full width at half-height) that was passed through a Wratten 88A infrared filter, to permit activation by light >700 nm. Photomultipliers were protected from the red flash excitation with Corning blue-green glass filters (9788) that do not significantly transmit light >630 nm). Data were accu-

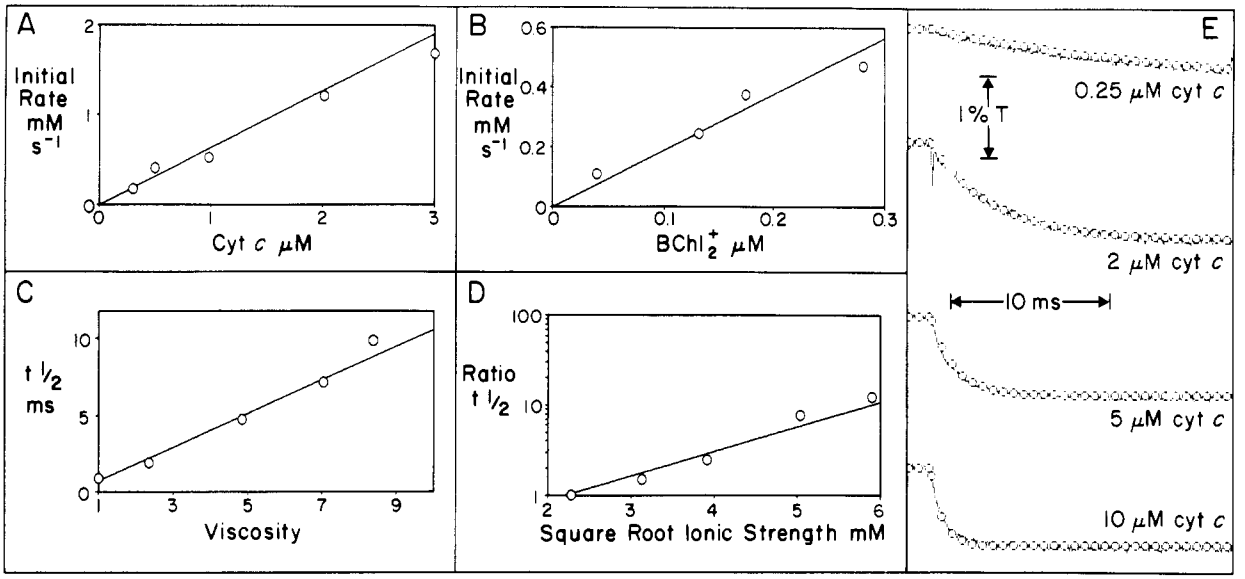

FIGURE 1: Cyt *c* oxidation at high ionic strength. (A) Effect of cyt *c* concentration on the initial rate of cyt *c* oxidation at 30 mM NaCl; 1 μM RC, 40% glycerol, and 10 mM Tris, pH 8. (B) Effect of $[BChl]_{2^+}$ concentration on the initial rate of cyt *c* oxidation at 30 mM NaCl; 1 μM RC, 2 μM cyt *c*, and 40% glycerol, pH 8. (C) Effect of viscosity on cyt *c* oxidation half-time at 30 mM NaCl; 1 μM cyt *c*, 1 μM RC, and 10 mM Tris, pH 8. (D) Effect of ionic strength on cyt *c* oxidation half-time relative to 0 mM NaCl; 1 μM RC, 2 μM cyt *c*, 40% glycerol, and 10 mM Tris, pH 8. (E) Cyt *c* oxidation kinetics at high salt and various cyt *c* concentrations: 550–540 nm; 30 mM NaCl, 0.5 μM RC, 40% glycerol, and 10 mM Tris, pH 8. Theoretical overlay: second-order kinetics, rate 1.4×10^8 M^{-1} s^{-1}.

mulated by using a Biomation Model 805 waveform recorder interfaced with an IBM personal computer.

Digital kinetic data were fit with nonlinear least-squares fitting routines developed for this purpose by adapting a Fortran general-fitting algorithm (Bevington, 1969) to include a flexible choice of kinetic types (first order plus second order, two first order, etc.) with the opportunity to free-fit or constrain any combination of parameters. Some reactions can be adequately fit by a single exponential, or a single exponential plus a constant. The successful fit of a series of kinetic traces, obtained at different concentrations and viscosities, to a single set of kinetic parameters often required the introduction of another phase, and both first-order and second-order phases were tried. The introduction of the second-order phase allows the trend of the kinetics to be followed with a single set of parameters except under conditions of significant product inhibition.

Spectral redox titrations were performed on a 200-Hz chopped-scanning dual-wavelength spectrophotometer interfaced with a dedicated PDP 11/10 computer that permitted averaging of spectra. In these measurements, redox mediator dye concentrations were increased to 10 μM, securing precise redox potential readings promptly.

RESULTS

The first experiments presented examine the cyt *c* oxidation kinetics in RC detergent suspension under a wide variety of conditions. With the appreciation gained from these experiments, parallel results are then presented of the analogous electron-transfer reactions with cyt c_2. Comparisons are then made with results obtained on cyt *c*–RC interactions when the RC is incorporated into neutral phospholipid vesicles. Finally, the effect on the cyt *c*–RC interaction of adding another membrane protein, cyt bc_1 complex or cyt *c* oxidase, is investigated.

In all experiments, kinetic activation was effected by a short, single-turnover flash. Unless stated otherwise, the intensity of the flash was sufficient to activate 90% of the RC population. This means that nearly all RC proteins are activated effectively at the same time. The light generates oxidized bacteriochlorophyll dimer ($[BChl]_{2^+}$) in the RC, and this serves to oxidize one ferrocytochrome *c*; once the RC has accepted an electron from cyt *c*, it removes itself from further participation in electron transfer. Thus, it is possible to observe the elementary first- and second-order reactions which reflect the detailed molecular dynamics unobscured by any multiple reaction of the RC.

The model used in the report is based on three states that can readily be distinguished by the singel-turnover approach (Overfield & Wraight, 1979, 1980a,b, 1986). The previously described "off", "distal", and "proximal" states are arranged as shown below, where k_a and k_{-a} are the association and

$$\text{off} \underset{k_{-a}}{\overset{k_a}{\rightleftarrows}} (\text{distal} \underset{k_{-b}}{\overset{k_b}{\rightleftarrows}} \text{proximal}) \xrightarrow{k_c} \text{cyt } c_{ox}$$

dissociation rate constants from and to the off state, respectively, k_b and k_{-b} are the forward and reverse rate constants, respectively, for conversion from the bound distal to the proximal state, and k_c is the rate of electron transfer from the proximal state.

Studies in Detergent RC Dispersion

Cyt c Kinetics at High Ionic Strength. Figure 1 shows that at the relatively high ionic strength of 30 mM NaCl, a simple viscosity-dependent second-order diffusional reaction is sufficient to effectively model the kinetic time course of cyt *c* oxidation. Panels A and B demonstrate that the electron transfer, whether measured by the initial rate of oxidation of cyt *c* or the coupled reduction of $[BChl]_{2^+}$, is linearly dependent on both reactant concentrations. Furthermore, panel C shows that the reaction half-time (which is inversely proportional to the rate constant) is linearly dependent on solution viscosity. Thus, the second-order rate constant, k_a, has an inverse dependence on the viscosity relative to water (η) with the form

$$k_a = k_d/\eta$$

where k_d is the rate constant at the viscosity of water. Panel D shows the relative half-time of the reaction is roughly proportional to the square root of the ionic strength, suggesting that the reactants act as oppositely charged species. Although

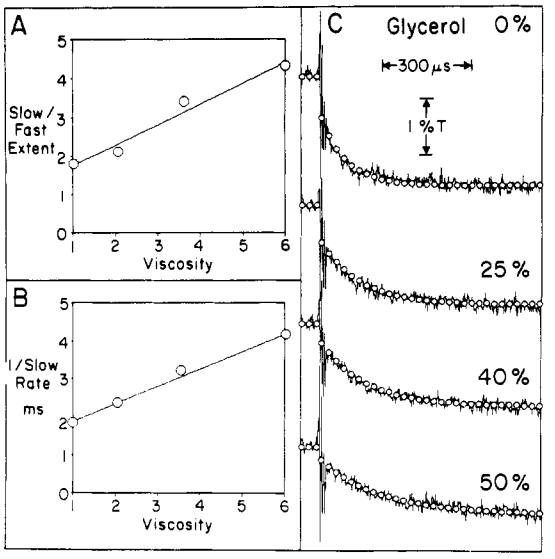

FIGURE 2: Effect of viscosity on cyt *c* kinetics at low ionic strength. (A) Effect on the slow to fast cyt *c* oxidation extents. (B) Effect on the slow cyt *c* oxidation rate. Both (A) and (B) contained 1 μM RC, 3.6 μM cyt *c*, and 10 mM Tris, pH 8, in the reaction medium the line represents the equation $1/k_b = (26\eta + 75)$ μs. (C) Cyt *c* oxidation kinetics at 0.5 μM cyt *c* and various glycerol concentrations: 1 μM RC and 10 mM Tris, pH 8; 550–540 nm. Open circles represent an unconstrained least-squares fit to a single exponential plus a constant. The noise at the break in kinetics is associated with a 8-μs half-width xenon flash. The slowest phase of the kinetics is visible in the longer time scale of panel A in Figure 3.

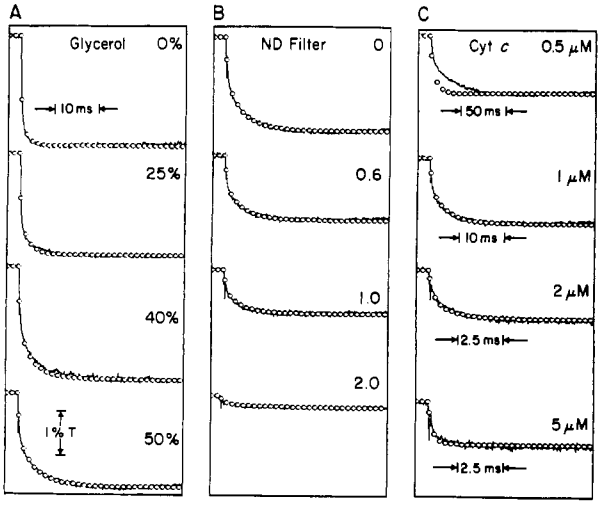

FIGURE 3: Cyt *c* oxidation kinetics under various conditions of viscosity, flash intensity, and cyt *c* concentration compared to predictions of the three-state kinetic model: 1 μM RC and 10 mM Tris, pH 8; 550–540 nm. (Panel A) 1 μM cyt *c*. (pAnel B) 1 μM cyt *c* and 40% glycerol. (Panel C) ND filter 0.6, 40% glycerol. Kinetic parameters: $k_a = 3 \times 10^9$ M^{-1} s^{-1}/η, $k_{-a} = 9 \times 10^2$ s^{-1}, $1/k_b = (2.6 \times 10^{-5})\eta + 7.5 \times 10^{-5}$ s, $k_{-b} = 1.8 \times 10^4$ s^{-1}.

this relationship can be described in terms of the Debye–Huckel theory, the derived charge product of −8.5 electron charge units squared is likely to be misleading. Other authors have shown that more sophisticated ionic strength dependence models for cyt *c* electron-transfer reactions are considerably more accurate (Koppenol et al., 1979; Rickle & Cusanovich, 1979). Finally, panel E confirms with four examples that a second-order time course based on these parameters can well describe the oxidation kinetics.

Cyt c Oxidation Kinetics at Low Ionic Strength. At low ionic strength, the multiphasic quality of cyt *c* oxidation is readily apparent; the analysis of these kinetics requires that two first-order-bound reactions be added to the relatively slow second-order reaction. In the biphasic kinetics captured on a 1-ms time scale in Figure 2, the time course of the faster proximal reaction is unresolved beneath the artifact associated with the approximately 8-μs half-width xenon flash. It is also apparent from the graphs of Figure 2 that a good linear fit to the viscosity dependence of both the rate and extent of the second, time-resolved phase (identified with the distal to proximal transition) can be achieved by the introduction of an inverse viscosity dependence of the rate of the distal to proximal reaction of the form

$$1/k_b = (26\eta + 75)\ \mu s$$

coupled with a viscosity-*independent* reverse reaction from the proximal to distal state of $k_{-b} = 1.8 \times 10^4$ s^{-1}. Note that these equations imply a finite rate of 1.4×10^4 s^{-1} for the distal to proximal reactions even at a theoretical solution viscosity of zero.

By use of a viscosity-dependent distal to proximal transition together with the second-order reaction observed at high ionic strength, Figure 3 demonstrates that it is now possible to fit the cyt *c* oxidation time course over a wide range of conditions using a single equation. A nonlinear least-squares fit to a theoretical time course of a second-order reaction plus a first-order reaction together with a constant, corresponding respectively to reaction from the off state, the distal state, and the proximal state, generates the following fit parameters shown in Table I: $k_a = 3 \times 10^9$ M^{-1} s^{-1}/η, $k_{-a} = 9 \times 10^2$ s^{-1}, $1/k_b = (2.6 \times 10^{-5})\eta + 7.5 \times 10^{-5}$ s, $k_{-b} = 1.8 \times 10^4$ s^{-1}. A sample of data and theoretical time courses using these parameters is shown in Figure 3; excellent fits are achieved.

Table I: Best-Fit Rate Constants[a]

system	k_a (M^{-1} s^{-1})	k_{-a} (s^{-1})	k_b (s^{-1})	k_{-b} (s^{-1})	K_D (μM)
RC–detergent–*c*	3×10^9	9×10^2	1×10^4	1.8×10^4	0.3
RC–detergent–c_2	1.5×10^8	1.6×10^2	2×10^3	1×10^3	1.1
RC–vesicle–*c*	3×10^9	7.5×10^2	1×10^4	3.2×10^4	0.5

[a] Best fits of flash-initiated electron-transfer kinetics to a three-state model described in the text, with the requirement that the rate constants remain the same over a range of cytochrome *c* and RC concentrations. Rates k_a and k_b exhibit an inverse dependence on solution viscosity. The reverse rates k_{-a} and k_{-b} are not observed directly but are derived from the extent of the forward phases assuming a preflash equilibrium between the forward and reverse rates.

Product Inhibition of Cyt c Oxidation. Although Figure 3 demonstrates that the three-state model succeeds in describing the kinetic time course under many conditions of concentration, viscosity, and flash intensity, the figure also shows a clear failure at low cyt *c* concentrations. While this might initially be interpreted as evidence of a very tight but slowly reacting cyt *c* binding site, such as that described by Dutton and Prince (1978) and Overfield and Wraight (1986), the following interpretation seems more valid. At low cyt *c* concentrations, as the electron transfer between RC and cyt *c* progresses, a significant amount of the total cyt *c* will become oxidized. If it was possible for cyt *c* to be oxidized by one RC, and then to rapidly dissociate and reassociate with another RC that has not yet reacted with reduced cyt *c*, then it may be able to inhibit that RC from participating in electron transfer. In other words, following diffusion of the oxidized cyt *c*, product inhibition might take place even after a single flash.

This hypothesis is confirmed by examining cyt *c* oxidation kinetics at different redox potentials. The top traces of Figure 4 represent flash kinetics at different redox potentials with different concentrations of oxidized cyt *c* present before the flash; the bottom traces have the corresponding reduced cyt *c* concentrations but with no oxidized cyt *c* present before the

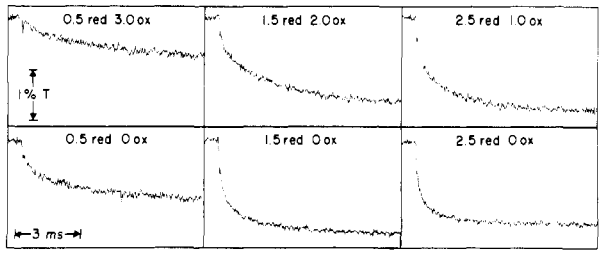

FIGURE 4: Cyt c oxidation in the presence and absence of preflash oxidized cyt c. (Top row) Total [cyt c] = 3.6 μM; the concentration of oxidized cyt c was adjusted by poising the redox potential at the appropriate values to obtain the quantities shown in the figure. (Bottom row) The E_h was poised at approximately 160 mV, where essentially all cyt c reduced before the flash: 1 μM RC, 50% glycerol, and 10 mM Tris, pH 8; 550–540 nm.

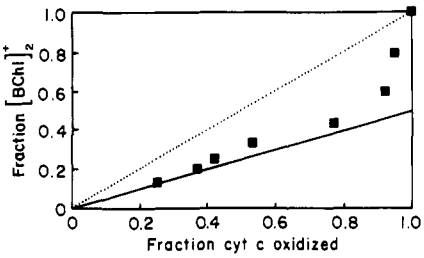

FIGURE 5: Fraction of the total cyt c oxidation extent presented as a function of different flash intensities. The data are plotted as the fraction of total $[BChl]_2^+$, generated by a flash of varying intensity, versus the amount of cyt c oxidized. The theoretical lines represent the behavior for completely "immobile" cyt c bound to RC (dotted) and for "mobile" cyt c, rapidly dissociating (solid). Maximum $[BChl]_2^+$ concentration, 1.4 μM; [cyt c], 0.7 μM; 10 mM Tris, pH 8, 10 μM Fe-EDTA, 10 μM 2-hydroxynaphthoquinone, and 0.5 μM diaminodurine; redox potential 150 mV; 550–540 nm.

flash. It is evident that inhibition by oxidized cyt c increases with preflash oxidized cyt c concentration.

The product inhibition model suggests not only rapid association and dissociation of oxidized cyt c but also comparable binding affinities for oxidized and reduced cyt c. The latter suggestion will be independently supported by redox titration data presented below.

Extent of Cyt c Oxidation at Cyt c:RC Ratios of Less Than Unity. Figure 5 shows the extent of cyt c oxidation at different flash intensities, and consequently different $[BChl]_2^+$ concentrations, in a solution in which the cyt c concentration has been adjusted to be half the RC protein concentration, i.e., half of the maximum concentration of $[BChl]_2^+$ created on the brightest (near-saturating) flash. Under these conditions, approximately 90% of the cyt c should be bound. Nevertheless, when the cyt c oxidation level is measured 200 ms after the flash, allowing time for the progress of the product-inhibited reaction to reach completion, it is found that most of the cyt c is oxidized at a flash intensity such that half of the RC is excited. This is expected of a reduced cyt c population that is mobile on a less than 100-ms time scale and is capable in this time period of reaching essentially all of the photoactivated RC. This mobility is in contrast to previous reports (Overfield et al., 1979; Overfield & Wraight, 1986).

Oxidation of Cyt c_2 in Detergent RC Dispersion. The oxidation of cyt c_2 by detergent-solubilized RC appears analogous to the oxidation of cyt c. At relatively low cyt c_2 concentrations, cyt c_2 also shows clear second-order oxidation kinetics with a linear viscosity dependence of the rate (data not shown). The zero glycerol rate of 1.5×10^8 M^{-1} s^{-1} is 20 times slower than the rate observed with cyt c. A reason for the slower rate of cyt c_2 oxidation may be due to its net charge at pH 8; the isoelectric point of cyt c_2 is 5.5 (Bartsch, 1971) whereas that

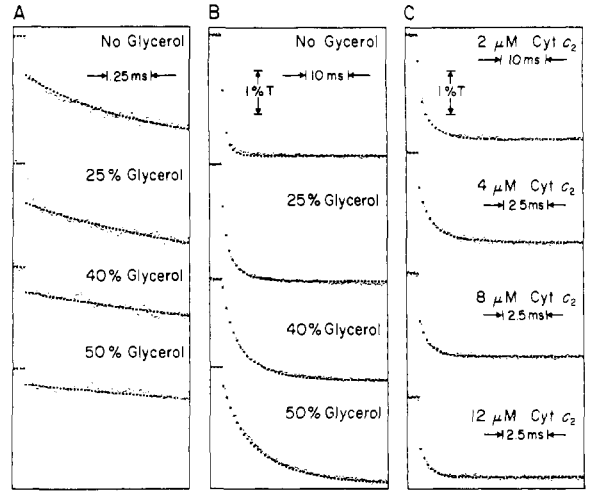

FIGURE 6: Cyt c_2 oxidation kinetics at different cyt c_2 and glycerol concentrations. (A and B) Glycerol concentration dependence of cyt c_2 oxidation at different time scales with the three-state theoretical overlay: 1 μM RC, 4 μM cyt c_2, and 10 mM Tris, pH 8; 550–540 nm. (C) Concentration dependence of kinetics; 1 μM RC and 10 mM Tris, pH 8. The overlay represents three-state theoretical kinetics with parameters of $k_a = 1.5 \times 10^8$ M^{-1} s^{-1}/η, $K_D = 1.1\eta$ μM, and $k_b = 2 \times 10^3$ s^{-1}/η.

of cyt c is 10.7 (Theorell & Akesson, 1941). Hence, cyt c_2 will have the same sign of net charge at pH 8 as the RC with an isoelectric point at 6.1 (Prince et al., 1974) and will not have the benefit of the monopole electrostatic attraction at a distance that appears to contribute to the relatively high collision and electron-transfer rate of the cyt c second-order diffusional reaction.

Once again, a relatively simple model of a viscosity-dependent second-order reaction plus a constant fast phase is insufficient to model the kinetic data under all conditions. It is essential to include an additional first-order reaction, corresponding to a distal bound cyt c_2, thus generating a three-state electron-transfer scheme similar to that found for cyt c. Figure 6 illustrates that the kinetics time course can be successfully modeled over a range of viscosities from 0% to 50% glycerol and from 2 to 12 μM cyt c_2 with the inclusion of a linearly viscosity-sensitive first-order rate of 2×10^3 s^{-1}. The K_D for cyt c_2 defined in terms of the unresolved fast phase and the first-order phase as bound states is 1.1η μM in the presence of 10 mM Tris-HCl. This is 3–4 times weaker than the binding of cyt c. This also may be a reflection of the difference in the sign of net charge of cyt c and cyt c_2. It is also found that under the same conditions the relative contributions of the unresolved fast phase and the first-order phase are approximately proportional to the cyt c_2 concentration but relatively independent of the solution viscosity.

Studies with Protein Reconstituted in Phosphatidylcholine Vesicles

Cyt c Binding to Lipid-Reconstituted RC. The cyt c oxidation kinetics observed with phosphatidylcholine-reconstituted RC are very similar to those described for LDAO-solubilized RC. However, redox titrations shown in Figure 7A demonstrate that the midpoint potential for cyt c in the presence of RC reconstituted via the dithionite reduction method (see Materials and Methods) into the neutral lipid vesicles is up to 40 mV lower than the midpoint for cyt c in buffer alone, cyt c in the presence of simple phosphatidylcholine vesicles, or cyt c in the presence of LDAO-solubilized RC protein. The replacement of LDAO by octyl glucoside via a cellulose-exchange column followed by reconstitution with phosphatidylcholine and dialysis (i.e., avoiding the dithionite reduction

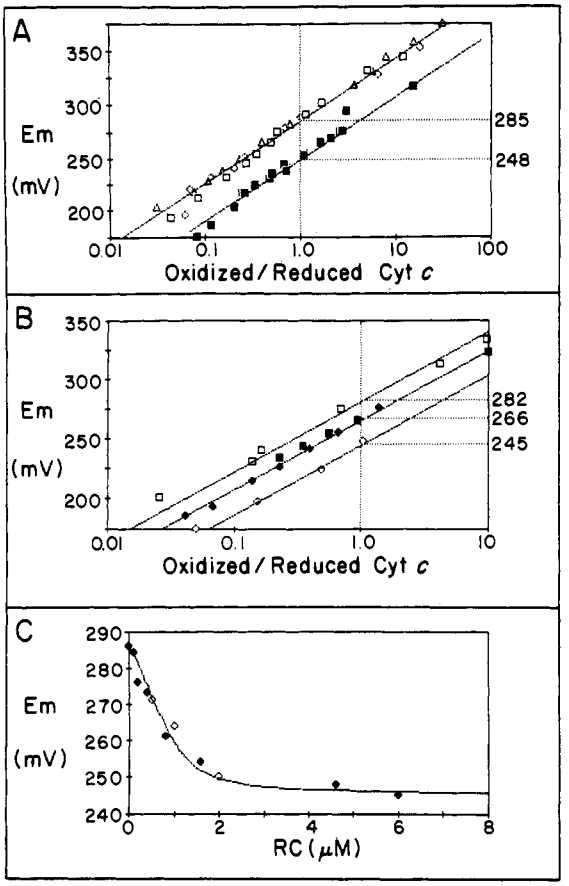

FIGURE 7: Midpoint of cyt *c* in the presence of vesicular RC protein reconstituted phosphatidylcholine vesicles. (A) Effect of lipid and RC on the redox midpoint of cyt *c*: (open diamonds) cyt *c* only; (open triangles) cyt *c* with lipid vesicles; (open squares) cyt *c* with RC solubilized in LDAO; (closed squares) cyt *c* in the presence of RC lipid vesicles. In all cases, the solution was buffered with 10 mM Tris-HCl, pH 8.0. (B) Effect of detergent on the redox midpoint of cyt *c*: (open diamonds) cyt *c* with RC vesicles; (closed diamonds) same conditions but with 0.1% Triton X-100; (closed squares) same conditions but with 0.3% Triton X-100; (open squares) cyt *c* with 0.5% Triton X-100 only. (C) Effect of RC vesicles on the redox midpoint of cyt *c*. Vesicles were prepared from RC originally solubilized in LDAO (open diamonds) or octyl glucoside (closed diamonds); 10 mM Tris, pH 8.0, and 4 μM cyt *c*. The theoretical lines are based on one or two binding sites.

strategy) generates a similar midpoint depression. Figure 7B shows that the addition of detergent to a phospholipid-reconstituted RC dispersion partially reverses the midpoint drop.

A model of unequal binding of reduced and oxidized cyt *c* to RC can relate dissociation constants to redox behavior. Consider the Nernst equations for the midpoint (E_m) of the unbound and bound cyt *c* (symbolized c_u and c_b, respectively):

$$E_h = E_{m_u} + 59 \log ([c^{ox}{}_u]/[c^{red}{}_u])$$

and

$$E_h = E_{m_b} + 59 \log ([c^{ox}{}_b]/[c^{red}{}_b])$$

and dissociation constants for RC protein binding oxidized and reduced cyt *c*

$$K_{D_{ox}} = N[RC][c^{ox}{}_u]/[c^{ox}{}_b]$$

and

$$K_{D_{red}} = N[RC][c^{red}{}_u]/[c^{red}{}_b]$$

where N is the number of cyt *c* binding sites per RC. The ratio of the reduced to oxidized dissociation constant is related to

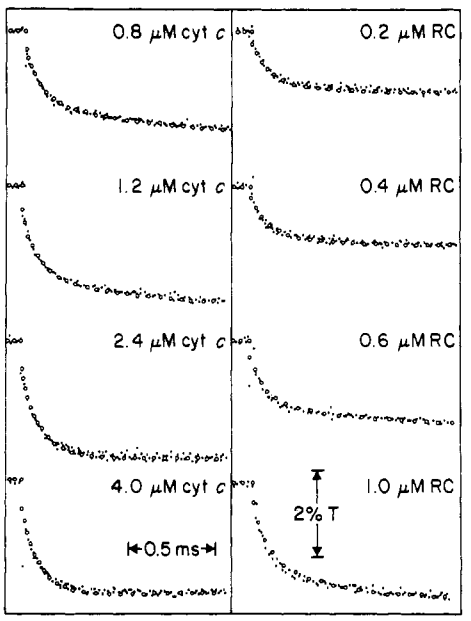

FIGURE 8: Cyt *c* oxidation by RC protein reconstituted lipid vesicles: [cyt *c*], 1 μM; [RC], 0.75 μM unless indicated. The theoretical points (open circles) follow a first-order rate of 1.0×10^4 s^{-1} plus a second-order rate of 3.0×10^9 M^{-1} s^{-1}, a first-order/constant extent = 3.2, K_D = 0.5 μM, and N = 2 independent binding sites.

the difference of the midpoints in the completely unbound and completely bound states by

$$E_{m_u} - E_{m_b} = 59 \log (K_{D_{red}}/K_{D_{ox}})$$

Thus, the midpoint drop of 40 mV translates into a 5-fold stronger binding by the RC of oxidized cyt *c* relative to reduced cyt *c*.

Equilibrium redox measurements permit a measure of the absolute value of the K_D for cyt *c* binding independent of the previously reported method involving centrifugal separation of vesicles from cyt *c* solution (Pachence et al., 1979a). Figure 7C shows the progressive drop in the cyt *c* midpoint as more and more phospholipid-reconstituted RC vesicles are added to the cyt *c* solution. By use of the above equations to calculate the E_h at which the total oxidized cyt *c* equals the total reduced cyt *c* (i.e., the experimental midpoint), the assumption of the number of binding sites and a K_D generates a theoretical curve (see appendix for derivation). The E_m of the data is found to fall too sharply with RC concentration to allow a fit to an N = 1 binding site. With N = 2, the K_D values for reduced and oxidized cyt *c* are 0.5 and 0.1 μM, respectively.

Kinetics of Cyt c Oxidation. If we now turn to fitting the cyt *c* oxidation kinetics by RC–lipid vesicles, we see that the redox-generated K_D = 0.5 μM, N = 2 parameters give almost the same ratio of unbound to bound RC as the kinetics-generated K_D = 0.27 μM, N = 1 parameters for the LDAO-solubilized RC. Figure 8 show some sample kinetics for cyt *c* oxidation by vesicular RC with a theoretical overlay using proximal, distal, and free cyt *c* states and similar rate constants as discovered with detergent dispersions of RC protein. The first-order rate from proximal to distal cyt *c* was increased from 1.8×10^4 to 3.2×10^4 s^{-1}, and the dissociation rate to "off" cyt *c* was decreased from 9.0×10^2 to 7.5×10^2 s^{-1}, relative to the detergent-solubilized system, to improve the fit.

It thus appears that the cyt *c* oxidation kinetics by RC protein in vesicles occur in much the same way as LDAO-solubilized RC protein, except that RC contained in the lipid reveals a higher affinity for oxidized cyt *c*. A consequence of such a higher affinity for the oxidized cyt *c* should be that this system will be more prone to the product inhibition. In-

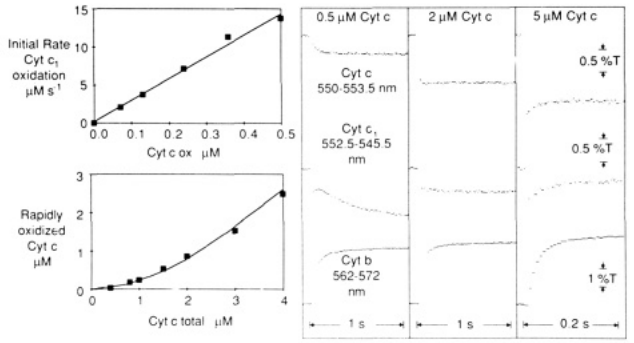

FIGURE 9: Flash-induced kinetics of the RC–cyt *c*–mitochondrial cyt bc_1 complex hybrid protein system. (Upper left) Initial rate of cyt c_1 oxidation measured at 552.5–545.5 nm; 0.5 μM $[BChl]_{2^+}$ maximum, 5 μM cyt *c*, 0.8 μM cyt bc_1 complex, 60% glycerol, 0.04% cholate, 20 μM each of antimycin, myxothiazol, and undecylhydroxynaphthoquinone, and 10 mM Tris, pH 8.0. Flash-oxidized cyt *c* concentration was adjusted by passing the xenon flash through neutral optical density filters. (Lower left) Inhibition of rapid cyt *c* oxidation in the presence of cyt bc_1 complex. Rapidly oxidized cyt *c* was measured at 550–553.5 nm 4 ms after the flash; 3.6 μM $[BChl]_{2^+}$, 1.5 μM cyt bc_1 complex, 20 μM antimycin, 0.04% cholate, and 10 mM Tris, pH 8.0. Theoretical fit for $K_D = 0.2\ \mu M$, where $K_D = [\text{cyt } c]_{\text{unbound}}[RC]_{\text{unbound}}/[\text{cyt } c]_{\text{bound}}$ and $[\text{cyt } c]_{\text{unbound}} = [\text{cyt } c]_{\text{oxidized}}$ by 4 ms. (Right) Flash-induced kinetics of critical redox centers under different cyt *c* concentrations. Concentrations as above.

deed, Figure 8 reveals the beginning of product inhibition in the form of slowed kinetics as the RC concentration is increased at low cyt *c* concentration.

Flash-Stimulated Cyt c Electron Transfer with Other Integral Membrane Proteins

The introduction of a second integral membrane protein to the RC–cyt *c* pair creates a RC hybrid protein system that carries the advantages of flash-activated electron transfer to the study of nonphotosynthetic proteins (Moser et al., 1986). The flash-activated kinetics of these systems define yet another bound cytochrome state that can be added to the three states already discussed.

A RC–Cyt c–Mammalian Cyt bc_1 Hybrid System. The right half of Figure 9 shows some examples of the flash-induced electron-transfer kinetics of a detergent-solubilized solution of RC protein, cyt *c*, and mitochondrial cyt bc_1 complex. Prior to activation, cyt *c*, cyt c_1, and the Rieske iron–sulfur center were poised-reduced. A flash of light creates an oxidized $[BChl]_{2^+}$ which in turn oxidizes cyt *c*. The top traces at 550–540 nm monitor this initial oxidation of cyt *c* by the flash-excited RC and its subsequent rereduction by the cyt bc_1 complex. After cyt c_1 has been oxidized by cyt *c*, the oxidizing equivalent is shared between the cyt c_1 and the Rieske iron–sulfur center. Subsequently ubiquinol, created by the photoevent within the RC, diffuses to a quinol oxidation site within the cyt bc_1 complex (Qz) and simultaneously donates one electron to the cytochromes *b* and another electron to the cyt c_1–Rieske iron–sulfur pair. Thus, the middle traces of Figure 9 at the wavelength pair 552.5–545.5 nm [chosen to monitor cyt c_1 exclusively, in analogy to Meinhardt and Crosts (1982)] reveal cyt c_1 oxidation upon donating an electron to the oxidized cyt *c*, and finally its rereduction by quinol. The bottom traces at 562–572 nm record the reduction of cyt *b* which is correlated with the quinol oxidation. At low cyt *c* concentrations, the relatively large residue of unreduced $[BChl]_{2^+}$ introduces a noticeable rapid downward spectral contribution to the cyt c_1 kinetics.

At sufficiently high cyt *c* concentrations, and with quinol oxidation by the cyt bc_1 complex inhibited by antimycin and myxothiazol, the rate of cyt c_1 oxidation displays the linear

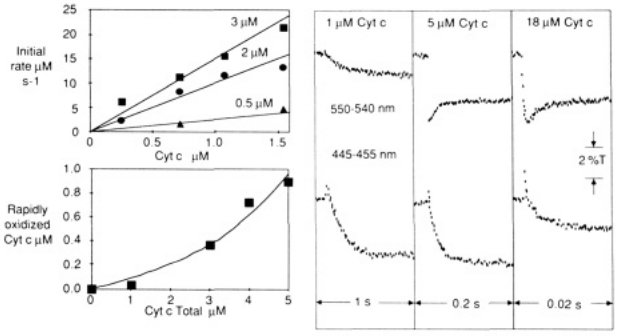

FIGURE 10: Flash-induced kinetics of the RC–cyt *c*–mitochondrial cyt *c* oxidase hybrid protein system. (Upper left) Initial rate of cyt *a* oxidation measured at 445–455 nm. Theoretical lines plotted for a second-order rate constant of 5 $\mu M^{-1}\ s^{-1}$. (Lower left) Amount of cyt *c* rapidly oxidized in the presence of 6 μM oxidase measured 10 ms after the flash; 2 μM RC, variable cyt *c* concentration, 0.5% cholate, 10 mM Tris, pH 8.0, and 10 μM each of 2-hydroxy-1,4-naphthoquinone and ferro-EDTA. Theoretical line represents $K_D = 0.5\ \mu M$. (Right) Flash-induced kinetics of cyt *c* and cyt *a* at different cyt *c* concentrations. Concentrations as above.

dependence on flash-oxidized cyt *c* concentration shown in the top left panel of Figure 9, as well as pronounced viscosity sensitivity (not shown) typical of a second-order diffusional reaction. However, at low cyt *c* concentration, the initial rate of cyt *c* flash oxidation by the RC is severely inhibited by the presence of the cyt bc_1 complex. The inhibition of rapid cyt *c* oxidation shown in the lower left panel is well described by a model of cyt *c* binding to the cyt bc_1 complex with a K_D of 0.2 μM and a dissociation rate somewhat faster than the 10 s^{-1} rate of cyt *c* oxidation in the limit of low cyt *c* concentrations. Also visible in the kinetics traces is the redox buffering effect of large concentrations of cyt *c* on the extent of cyt c_1 oxidation. This is expected of a reversible electron-transfer reaction between two redox centers with relatively similar redox midpoint potentials.

A RC–Cyt c–Cyt c Oxidase Hybrid System. Figure 10 shows a parallel kinetics situation in the detergent-solubilized solution of RC, cyt *c*, and mitochondrial cyt *c* oxidase. All hemes were poised initially reduced before the flash excitation. Upon activation, the RC creates oxidized $[BChl]_{2^+}$, which then oxidizes cyt *c*. The top kinetics traces in this figure follow this cyt *c* oxidation by the RC and its subsequent reduction by the oxidase. The bottom traces at 445–455 nm follow the resultant cyt *a* oxidation by the cyt *c*. Note we are here promoting an electron transfer through the oxidase opposite to the net physiological direction. The top right panel describes the analogous linear dependence of the cyt *a* oxidation rate on the concentration of the reactants, flash-oxidized cyt *c* and reduced oxidase, expected of a second-order diffusional reaction. In analogy with the RC–cyt bc_1 complex hybrid system, cyt *c* oxidation by the flash-excited RC at low cyt *c* concentrations is severely inhibited by the presence of the oxidase. The pattern of rapid cyt *c* oxidation as a function of cyt *c* concentration is also well modeled by a binding site, but with a K_D on the oxidase of 0.5 μM and a dissociation rate that is faster than the 8 s^{-1} limit of cyt *c* oxidation observed at the low cyt *c* concentration. This K_D is in the range of reported equilibrium and steady-state kinetics binding constant values (Ferguson-Miller et al., 1976). The redox buffering effect of large concentrations of cyt *c* on the extent of cyt *a* oxidation is also evident from the kinetics.

DISCUSSION

The modeling of flash-induced cyt *c* oxidation kinetics confirms the following conclusions: (1) the three-state model

with off, distal, and proximal states is essentially correct, and (2) electrostatic interactions are of primary importance. Furthermore, such modeling indicates that (3) the binding and mobility of oxidized cyt *c* can lead to a profound product inhibition, (4) the exchange dynamics of oxidized and reduced cyt *c* are similar regardless of the state of activation of the RC, (5) preferential binding of the oxidized form of cyt *c* is revealed upon reconstitution of RC into neutral lipid, independently confirming the binding suggested by the kinetics, and (6) the viscosity sensitivity of the bound-state reactions has important orientational and energetic implications.

Validity of the Three-State Model. A three-state model of RC–cyt *c* interaction is the minimal model required for an adequate description of the kinetics time course of electron transfer from ferrocytochrome *c* or c_2 to flash-oxidized $[BChl]_2^+$. Unassociated cyt *c* and RC participate in a viscosity-dependent second-order collisional reaction leading to two distinguishable bound states. The apparent second-order rate constant calculated for this reaction at low ionic strength and at the viscosity of water is 3.3×10^9 M^{-1} s^{-1}, surprisingly close to the theoretical rate limit of about 5×10^9 M^{-1} s^{-1} for the action of diffusing spheres reactive over their entire surfaces, using RC and cyt *c* diffusion constants of 5×10^{-7} and 13×10^{-7} cm^2 s^{-1} (Rivas et al., 1980; Margoliash & Listgarten, 1962) substituted into Smoluchowski's diffusion equation (von Smoluchowski, 1917):

$$k = 4\pi(r_A + r_B)(D_A + D_B)10^{-3}N_0$$

where k is the second-order rate, r is the radius of each of the colliding A and B molecules, D is the diffusion coeffic ient, and N_0 is Avogadro's number.

Importance of Electrostatics. Given the ionic strength dependence of this second-order reaction, it seems clear that part of the relative rapidity of this reaction can be explained by an electrostatic guidance. The isoelectric points of cyt *c* at 10.7 (Theorell & Akesson, 1941) and RC at 6.1 (Prince et al., 1974) lead to oppositely charged species at pH 8, and a monopole electrostatic attraction should lead to more frequent interaction. In addition, the relatively large cyt *c* electric dipole of 300 D (Koppenol & Margoliash, 1982) should lead to a higher orientation on collision and accelerate electron-transfer kinetics in a fashion similar to that shown by Margoliash and co-workers for the steady-state electron-transfer reactions of modified lysine derivatives of cyt *c* with the mitochondrial proteins cyt *c* oxidase and cyt bc_1 complex (Koppenol & Margoliash, 1982; Speck & Margoliash, 1984; Speck et al., 1984; Margoliash & Bosshard, 1983).

When considering the electrostatic interactions between cyt *c* and RC, an ideal description will include the spatial distribution of all the partial charges in both proteins and the effects of the dielectrics within and without the proteins [see, for example, Northrup et al. (1986)]. These details of the charge distribution are likely to be very important when the proteins are in contact. Nevertheless, the considerably simpler view of the electrostatic properties of cyt *c* or cyt *c* as a superimposed charge monopole and dipole permits an approximation of the electrostatic interaction between cyt *c* (or cyt c_2) and RC at large distances and may still be valuable when the proteins are close together.

Product Inhibition on a Rapid Time Scale. An entirely unexpected result of this analysis is that oxidized cyt *c* appears to bind to activated RC and, during its tenure, physically block reduced cyt *c* from electron transfer. Kinetics and redox data are consistent with a rapid dissociation and association of both oxidized and reduced cyt *c* with nearly equal binding affinity by detergent-solubilized RC. Thus, oxidized cyt *c* formed immediately after a flash has the opportunity to migrate to unreacted RC and inhibit electron transfer. The removal of detergent and the reconstitution of RC into neutral lipid reveal a preferential binding of RC for oxidized cyt *c* that is not associated with the lipid itself. This apparently contributes to an enhanced product inhibition by binding oxidized cyt *c* more than reduced cyt *c* but maintaining a relatively rapid rate of dissociation and association of oxidized cyt *c*.

Constant Exchange Dynamics with Activated and Unactivated RC. It is clear from the single-turnover product inhibition that oxidized cyt *c* must dissociate relatively rapidly (on a 10-ms time scale) from reduced RC. Given the absence of an E_m drop for cyt *c* in the presence of detergent-solubilized RC, and hence the similarity of binding of oxidized and reduced cyt *c* ot the RC, this suggests that reduced cyt *c* may dissociate on a similar time scale. Figure 5 confirms this suggestion. In a solution with a cyt *c* concentration of half the $[BChl]_2^+$ concentration at maximum flash intensity, a condition in which most cytochrome should be bound, substantially less that all the $[BChl]_2^+$ must be excited in order to oxidize nearly all the cyt *c* in solution, as measured 200 ms after the flash. Reduced cyt *c* thus dissociates and becomes mobile on the time scale of electron-transfer kinetics.

This result is in contrast to similar experiments in which it was shown that almost all the $[BChl]_2$ was apparently required to be flash activated to oxidize all of a substoichiometric concentration of cyt *c* or cyt c_2 (Overfield et al., 1979; Overfield & Wraight, 1986). Their conclusion was that an unactivated RC and cyt *c* can maintain a long-lived complex with a dissociation rate more than 100 times slower than that for activated RC and that such a bound state of cyt *c* persists even at 100 mM NaCl. The conflict between the data might be reconciled if the estimation of the extent of cyt *c* oxidation on a rapid time scale in the Overfield and Wraight experiments neglected the relatively slow product-inhibited kinetics. An underestimation of cyt *c* oxidation extent at near-saturating light levels, where product inhibition is most severe, may have distorted the results which led to the description of relatively immobile reduced cyt *c*. The necessity for an ionic strength insensitive bound state disappears when product inhibition is recognized.

Preferential Binding of Oxidized Cyt c in Vesicular RC. Although the kinetics of cyt *c* oxidation by RC reconstituted into neutral phosphatidylcholine vesicles can be described by a similar three-state model as the detergent-solubilized RC, vesicular RC displays a 5-fold stronger binding for oxidized relative to reduced cyt *c*, as reflected in a midpoint potential drop of up to 40 mV. A preferential binding of the oxidized form of cyt *c* has also been reported with purified cyt *c* oxidase (Vanderkooi & Erecinska, 1974) and cyt bc_1 complex (Speck & Margoliash, 1984). The appearance of redox state sensitive binding in vesicular RC may reflect the removal of obscuring detergent from the RC surface.

The concentration dependence of this midpoint drop indicates that there are at least two binding sites specific to the RC reconstituted into lipid membranes, consistent with the values of two to three binding sites reported by Pachence et al. (1979a) in RC proteoliposome sedimentation studies. On the other hand, the minimum number of binding sites required by the kinetics modeling is 1, if one assumes exclusive binding of cyt *c* in a distal or proximal orientation. The kinetics model can accommodate a larger number of binding sites provided that the average K_d is weakened and thus the overall concentration dependence of the bound vs unbound cyt *c* ratio is maintained. This is the change found as the kinetics-derived

$N = 1$ binding site value of 0.27 μM is weakened to the E_m drop derived $N = 2$ value of 0.5 μM. Although the number of binding sites on the RC is not entirely clear under all conditions, a value of two to three binding sites is consistent with most observations.

Viscosity Sensitivity and Orientational Implications. The modeled kinetics reveal a surprising viscosity sensitivity in that the distal bound state can be converted to a proximal state in a viscosity-dependent first-order reaction, with the reverse reaction having a significantly lesser or zero viscosity dependence. The viscosity dependence of the distal to proximal reaction suggests that distal cyt *c* must undergo a viscosity-sensitive translational and/or rotational diffusion to enter an optimal (proximal) bound state orientation that promotes relatively rapid electron transfer. A priori, a viscosity-sensitive distal to proximal reaction would be expected to be accompanied by a similarly viscosity-sensitive proximal to distal reaction, and hence a viscosity-insensitive distal/proximal partition, contrary to observation. Strong orientational constraints in the proximal state and electrostatic attractions in the distal state may serve to make the microscopic motions of the proximal to distal reaction less likely to be immediately reversed, thus decreasing the "cage effect" (Benesi, 1984) and hence the viscosity sensitivity of this reaction.

Another view of the relative orientation of the bound states has been described by Tiede (1985, 1987). In oriented neutral lipid-reconstituted RC membranes, the absorption change associated with cyt *c* oxidation in the fast (proximal) phase, but not the slow (distal) phase, was found to be dichroic. Thus, a relatively constrained orientation of cyt *c* at the proximal (but not necessarily distal) site was defined with a geometry that suggests that the heme edge is relatively close to the RC surface. The lack of dichroism of the distally positioned cyt *c* does not allow discrimination between the possibilities of a distal cyt *c* heme normal that is (a) unoriented or (b) highly oriented at an angle around 55°; it is also silent on the question of translation between distal and proximal cyt *c*.

Model of Distal-State Minimum Energy Electrostatics. A synthesis of the electrostatic and orientational pictures can be found in the following model for the physical distinctions between the distal and proximal states. Besides the different net charges of cyt *c* and RC which can accelerate the second-order collisional reaction by a strong monopole attraction, the strong dipole of cyt *c* will also orient toward its reaction partner. However, it has been noted (Koppenol & Margoliash, 1982) that the intersection of the dipole with the cyt *c* protein surface is not exactly at the location where the heme edge reaches the surface and where electron transfer most probably occurs. Instead, the dipole is oriented 33° off the plane of the heme and the heme crevice. Our model contends that the distal state corresponds to the most favorable electrostatic position, with the cyt *c* dipole oriented directly toward the RC, and that a rotational motion (suggested by the viscosity and dichroic data) involving work against the electrostatic attraction is required to reorient the cyt *c* such that the heme edge is in a favorable orientation for the rapid electron transfer defining the proximal site.

Such a model explains the zero viscosity extrapolated rate of cyt *c* oxidation. Even without viscosity-dependent drag, a certain amount of thermal energy, and hence a certain amount of time, would be required to work against the electrostatic attraction of the distal bound cyt *c* and orient it for electron transfer. A rough estimate of the electrostatic energies (U) involved can be derived by using the equation:

$$U = \mu E(1 - \cos \theta)$$

Substituting with the values of $\theta = 33°$ and $\mu = 300$ D for the orientation and strength of the cyt *c* dipole, and using an estimated electric field strength (E) based on that suggested for the cyt *c* binding site of the bc_1 complex of 18×10^6 V/m (Koppenol & Margoliash, 1982), generates an activation energy of 0.4 kcal/mol, compared with about 0.6 kcal/mol for the room temperature thermal energy. Thus, the energy associated with the electrostatic work of moving the cyt *c* dipole from its most favored electrostatic position to an electron-transfer position may be in a range that can influence the reaction rates and could potentially explain the origin of distal and proximal states and from them the observed electron-transfer rates.

The proposed model of distal-state cyt *c* binding suggests that the intersection of the cyt *c* dipole with the cyt *c* surface, found approximately in the middle of the triangle formed by lysines-13, -72, and -86 (Koppenol & Margoliash, 1982), should point toward the RC. Such an orientation is similar to that described by Tiede (1987) for the weakly dichroic binding of cyt *c* to oriented negatively charged vesicles. Thus, our model contends that the weak or absent dichroism of distal cyt *c* oxidation is due predominantly to its orientation at 55°, although the dichroism may also be weakened due to the translation and rotation associated with the multiple cyt *c* binding sites suggested by the redox titration data.

Parallels to Cyt c_2 Oxidation. As with cyt *c* oxidation, cyt c_2 oxidation by RC fits a three-state model, although there are some differences in detail. The second-order reaction rate for cyt c_2 is similarly inversely dependent on viscosity. However, the second-order rate constant of 1.5×10^8 M^{-1} s^{-1} is 20 times slower than that for cyt *c* oxidation, consistent with the absence of a monopole electrostatic attraction between the RC and the similarly charged cyt c_2, which has an isoelectric point of about 5.5 (Bartsch, 1971). The rate is somewhat slower than a previously reported rate of 7×10^8 M^{-1} s^{-1} (Overfield & Wraight, 1979). Partly as a reflection of this decreased rate, our K_D for cyt c_2 binding is weaker.

We find the first-order reaction rate from the distal state is also inversely viscosity sensitive, once again suggesting a similar rotational and/or translational diffusion to the proximal state. However, the cyt c_2 distribution between the distal and proximal states is less affected by viscosity than the cyt *c* distribution. If the distal state corresponds to a low-energy electrostatic orientation, then this could mean that the cyt c_2 dipole is weaker than the cyt *c* dipole or that the difference in orientation between the cyt c_2 distal and proximal states is less than that for cyt *c*. A direct comparison of the electrostatic potential surfaces of cyt *c* and cyt c_2 (Weber & Tollin, 1985) shows a roughly similar orientation of the positive surface near the heme edge, although the surface for the net positively charged cyt *c* is considerably larger than that evident for cyt c_2. Viscosity-sensitive electron-transfer kinetics were previously reported with cross-linked cyt *c*–RC complexes; in contrast, the cross-linked cyt c_2–RC complex was found to be viscosity insensitive (Rosen et al., 1983).

The cyt c_2 distal to proximal rate of 2×10^3 s^{-1} is about 5 times slower than that found for cyt *c* oxidation and similar to a previously reported rate (Overfield & Wraight, 1979). Unlike cyt *c*, the cyt c_2 distal/proximal partion displays a clear sensitivity to the cyt c_2 concentration. This is the only evidence provided here for multiple binding to the RC. Such multiple binding is consistent with the theoretical multiple-turnover considerations considered below.

A rigorous examination of an in vivo E_m drop for cyt c_2 has not been done, due to earlier confusion of redox data with the

presence of cyt c_1 (Dutton et al., 1975; Bowyer et al., 1979). We did not test cyt c_2 with the RC phospholipid vesicles in the present work.

Advantages of Distal-State Binding. The distal/proximal cyt *c* partition may find its physiological significance as an evolutionary refinement of the electron-transfer scheme to assure maximal rates of multiple turnover in vivo. In particular, maximal electron transfer throughout should occur if both association and dissociation rates of cyt *c* and RC are also maximal. However, cyt *c* is not able to transfer electrons isotropically, but instead requires a specific orientation. The binding energy well associated with an oriented cyt *c* will decrease the dissociation rate. At the extreme case, the product, oxidized cyt *c*, will choke multiple turnover flow by remaining attached to the electron-transfer site. (Indeed, the observation of product inhibition suggests this tendency.) Mutational changes which allowed the selective rapid dissociation of oxidized cyt *c* would encourage multiple turnover and might be favored. However, such changes would have the effect of decreasing the free energy of electron transfer by raising the midpoint of cyt *c* and run contrary to the midpoint drop seen with vesicular cyt *c*.

An alternative mutational change which electrostatically attracted cyt *c* to multiple binding sites near the electron-transfer site would, by competition, help clear the electron-transfer site for the next cyt *c* and would have the additional advantage of effectively increasing the local cyt *c* concentration. Thus, creation of distal sites might be favored by natural selection.

It is of considerable interest that cyt c_2 has been shown *not* to be absolutely essential for the electron transfer between RC and bc_1 complex; some mutants devoid of cyt c_2 survive in the laboratory (Daldal et al., 1986). However, they do not compete with wild-type strains and would not be expected to survive in natural settings. Thus, cyt c_2 represents a significant improvement over direct electron transfer from the cyt bc_1 complex to the RC, and the introduction of a distal/proximal cyt c_2 arrangement may represent a further refinement. The refinement of multiple distal cyt *c* binding sites may have been carried to an extreme in the RC of photosynthetic bacteria such as *Rhodopseudomonas viridis* where a linear array of four cyt *c* hemes are fixed in a hydrophobic subunit of the RC structure (Deisenhoffer et al., 1985). Thus, the water-soluble cyt c_2 in redox contact with the fixed hydrophobic hemes of the RC found in *Rp. viridis* and many similarly equipped bacteria may have no need for the distal/proximal partition conspicuous in *Rhodobacter sphaeroides* and *Rb. capsulatus*; this remains to be investigated.

Analogies to Other Protein Systems. The apparent participation of translational and rotational motion in electron transfer between cyt *c* (c_2) and RC finds a parallel in the reaction between cyt *c* and other proteins. Kinetic experiments with naturally occurring variants of eukaryotic cyt *c*, with single lysine modification of cyt *c*, as well as residue shielding experiments on bound cyt *c* suggest that an extensively overlapping portion of the cyt *c* surface is involved in binding to mitochondrial bc_1 complex and cyt *c* oxidase and imply the participation of at least the motion of cyt *c* dissociation and reassociation in electron transfer between the complexes (Speck et al., 1979; Reider & Bosshard, 1980; Ahmed et al., 1978; Smith et al., 1980; Konig & Osherhoff, 1980). Indeed, the current paper shows the inhibition of rapid cyt *c* oxidation in the presence of mitochondrial cyt bc_1 complex or cyt *c* oxidase, with a concentration dependence that strongly suggests cyt *c* binds more strongly to these proteins than to the RC. Rapid oxidation of cyt *c* by the RC under such a bound condition appears to be impossible; the process is best described by the sequence of cyt *c* dissociation from these proteins, followed by cyt *c* diffusion, binding to the RC, and then oxidation by the RC.

Because the engineering problems addressed for multiple-turnover cyt *c* oxidation in the RC system are just as much a concern for cyt oxidase, we might expect a similar kinetics and mechanism for the two systems. Indeed, besides evidence for significant product inhibition (Minnaert, 1961; Speck et al., 1984; Sinjorgo et al., 1984) and preferential binding of oxidized cyt *c* (Vanderkooi & Erecinska, 1974), cyt oxidase has shown multiphasic cyt *c* oxidation kinetics (Andreasson et al., 1972; Wilson et al., 1975) and binding of two *c* cytochromes (Ferguson-Miller et al., 1976, 1978; Brautigan et al., 1978). The steady-state kinetics have also been shown to be nonhyperbolic (Nicholls, 1965; Errede et al., 1976; Ferguson-Miller et al., 1976). Some authors have argued that a second cyt *c* binding site can generate multiphasic kinetics and nonhyperbolic steady-state behavior through direct electron transfer (Ferguson-Miller et al., 1978; Errede & Kamen, 1978) or by an indirect regulation (Speck et al., 1984; Sinjorgo et al., 1986). Still others suggest that the kinetics do not require multiple binding sites but can be generated by conformational changes of the oxidase associated with the succession of oxidation states during the four-electron reduction of oxygen (Antalis & Palmer, 1982; Brezezinski et al., 1986) or by a cyt *c* to *c* relay electron transfer (Malmstrom & Andreasson, 1985).

The cyt *c*–RC model is most similar to the indirect regulation model described by Speck et al. (1984) in that it suggests a single electron-transfer site in which activity is enhanced by adjacent binding sites, and consequently shares the same success in explaining the multiple binding and multiphasic kinetics data under both single-turnover and multiple-turnover conditions. The similarity of the models increases if it is supposed that a rapid equilibrium occurs between the oxidase binding sites. However, the cyt *c*–RC model does not suggest that dissociation of ferricyt *c* is necessarily rate limiting for cyt *c* oxidation, in that ferricyt *c* may remain at a distal site only partially inhibiting further cyt *c* oxidation. Thus, the mechanism for turnover in the presence of a slowly dissociating ferricyt *c* from an electron-transfer site could be due to a distal binding pull on ferricyt *c* rather than a distal push from a concurrently bound reduced cyt *c*. It remains to be resolved if the orientational and electrostatic aspects of the proximal–distal cyt *c*–RC model are valid with the oxidase (Speck et al., 1984). In drawing parallels between RC and cyt *c* oxidase, it should be kept in mind that the binding of cyt *c* to cyt *c* oxidase described as a high-affinity binding may be associated with a single cyt *c* binding to a proximal or distal site and that a low-affinity binding may be associated with multiple cyt *c* binding.

Final Comments. The detailed study of the RC–cyt *c* interactions permitted by flash-activated single-turnover electron transfer reveals a kinetics system in which a simple second-order diffusional reaction under conditions of high ionic strength becomes enhanced by binding at lower ionic strengths to exhibit a combination of diffusional second-order and both diffusional and nondiffusional first-order electron-transfer kinetics. The multiple binding, biphasic kinetics, and orientational properties of the bound states begin to suggest a well-choreographed style of molecular engineering that maintains maximum rates of multiple turnover that could be generally applicable to interactions between cyt *c* and several

major electron-transfer proteins.

Over the past 30 years, approaches aimed at describing these manifold levels of cyt *c* function have been applied to detergent-solubilized and phospholipid-reconstituted preparations as well as to unaltered native material. Our studies here have demonstrated that the preparation-dependent results from the isolated proteins can be rationalized under one model mechanism. It is also clear that in studies using native material, the investigation of a detailed mechanism of a specific cyt *c*–protein interaction can be easily obscured by the membrane and other cyt *c* binding proteins. The approach to a complete functional description is best made through stages that progress from protein-reconstituted (hybrid) systems finally to native systems for viewing the integrated physiological performance of the distinct functional details. It is natural to expect that future studies with cyt *c* and cyt c_2 analogues will reveal more of the molecular dynamics of the fine electrostatic interaction.

ACKNOWLEDGMENTS

We are happy to acknowledge stimulating and very helpful discussions with Colin A. Wraight and Shelagh Ferguson-Miller.

APPENDIX

Concentration Dependence of Binding-Induced Midpoint Potential Drop. The desired expression relates the observable total RC and cyt *c* concentrations ($[RC]_{tot}$ and $[c]_{tot}$, respectively) to the experimental midpoint potential (E_h), given the theoretical RC dissociation constants for oxidized and reduced cyt *c* (K_{D_o} and K_{D_r}, respectively) and the number of identical binding sites per RC (N).

Nernst equations can be written in terms of the cyt *c* species concentrations: oxidized and reduced bound cyt *c* ($[c]_{o_b}$ and $[c]_{r_b}$, respectively) with redox midpoint potential E_{m_b}, as well as oxidized and reduced unbound cyt *c* ($[c]_{o_u}$ and $[c]_{r_u}$, respectively) with redox midpoint potential E_{m_u}:

$$[c]_{o_b}/[c]_{r_b} = 10^{E_h - E_{mb}/59} \equiv B \quad \text{(A1)}$$

$$[c]_{o_u}/[c]_{r_u} = 10^{E_h - E_{mu}/59} \equiv U \quad \text{(A2)}$$

where B and U are shorthand symbols for the bound and unbound exponential terms, respectively. At the experimental midpoint, the concentrations of oxidized and reduced cyt *c* are equal, by definition:

$$[c]_{o_b} + [c]_{o_u} = [c]_{r_b} + [c]_{r_u} = [c]_{tot}/2 \quad \text{(A3)}$$

The definition of the dissociation constant for reduced cyt *c* includes the term for the number of free RC binding sites, equal to N times the total RC concentration minus the number of cyt *c* bound ($[c]_{b_{tot}}$):

$$K_{D_r} = (N[RC]_{tot} - [c]_{b_{tot}})[c]_{r_u}/[c]_{r_b} \quad \text{(A4)}$$

which can be rewritten

$$[RC]_{tot} = (1/N)(K_{D_r}[c]_{r_b}/[c]_{r_u} + [c]_{b_{tot}}) \quad \text{(A5)}$$

To write the ratio $[c]_{r_b}/[c]_{r_u}$ in terms of knowns, note from eq A3 that

$$[c]_{o_u} - [c]_{r_u} = [c]_{r_b} - [c]_{o_b} \quad \text{(A6)}$$

and from eq A1 and A2

$$[c]_{r_b}(1 - B) = [c]_{r_u}(U - 1) \quad \text{or} \quad [c]_{r_u}/[c]_{r_b} = (1 - B)/(U - 1) \quad \text{(A7)}$$

It only remains to write $[c]_{b_{tot}}$ in terms of knowns. By definition:

$$[c]_{b_{tot}} = [c]_{o_b} + [c]_{r_b} \quad \text{(A8)}$$

Substitution of eq A1 and rearrangement imply

$$[c]_{o_b} = [c]_{b_{tot}}[B/(1 + B)] \quad \text{(A9)}$$

Similarly

$$[c]_{o_u} = [c]_{u_{tot}}[F/(1 + F)] \quad \text{(A10)}$$

with the sum, as in eq A3

$$[c]_{tot}/2 = [c]_{b_{tot}}[B/(1 + B)] + [c]_{tot} - [c]_{b_{tot}}[F/(1 + F)] \quad \text{(A11)}$$

where $[c]_{u_{tot}}$ has been substituted by $[c]_{tot} - [c]_{b_{tot}}$.

Solving for $[c]_{b_{tot}}$ gives

$$[c]_{b_{tot}} = [c]_{tot}(1 - F)(1 + B)/2(B - F) \quad \text{(A12)}$$

Substituting in eq A5 gives

$$[RC]_{tot} = (1/N)\{K_{D_r}(U - 1)/(1 - B) + [c]_{tot}(1 - F) \times (1 + B)/[2(B - F)]\} \quad \text{(A13)}$$

This equation describes the theoretical lines of Figure 7. Note that even with an infinitely strong binding constant, if there is only a single binding site ($N = 1$), then the theoretical midpoint will not fall fast enough with the RC concentration to fit the data. Multiple binding sites permit a fit.

The presence of bound and unbound cyt *c* leads to an oxidized/reduced cyt *c* vs redox potential behavior that is not strictly linear on a log plot, unlike the Nernst behavior observed with a single redox species. However, if the difference in midpoint potential between the bound and unbound species is less than 60 mV (as it is here), then the nonlinearity results in a slope deviation of only a few percent and does not interfere with an accurate midpoint determination.

Registry No. Cyt *c*, 9007-43-6; cyt c_2, 9035-43-2; ubiquinol–cyt-*c* oxidoreductase, 9027-03-6; cyt *c* oxidase, 9001-16-5.

REFERENCES

Ahmed, A. J., Smith, H. T., Smith, M. B., & Millett, F. S. (1978) *Biochemistry 17*, 2479–2483.

Andreasson, L. E., Malmstrom, B. G., Stromber, C., & Vanngard, T. (1972) *FEBS Lett. 28*, 297–301.

Antalis, T. M., & Palmer, G. (1982) *J. Biol. Chem. 257*, 6194–6206.

Bartsch, R. G. (1971) *Methods Enzymol. 23*, 344–363.

Benesi, A. J. (1984) *J. Phys. Chem. 88*, 4729–4735.

Bevington, P. R. (1969) *Data Reduction and Error Analysis for the Physical Sciences*, McGraw-Hill, New York.

Bowyer, J. R., Tierney, G. V., & Crofts, A. R. (1979) *FEBS Lett. 101*, 207–212.

Brautigan, D. L., Ferguson-Miller, S., & Margoliash, E. (1978) *Methods Enzymol. 53*, 128–164.

Brezezinski, P., Thornstrom, P. E., & Malmstrom, B. G. (1986) *FEBS Lett. 194*, 1–5.

Clayton, R. K., & Wang, R. T. (1971) *Methods Enzymol. 23*, 696–704.

Daldal, F., Cheng, S., Applebaum, J., Davidson, E., & Prince, R. C. (1986) *Proc. Natl. Acad. Sci. U.S.A. 83*, 2012–2016.

Deisenhoffer, J., Epp, O., Miki, K., Huber, R., & Michel, H. (1985) *Nature (London) 318*, 618–624.

Dutton, P. L. (1978) *Methods Enzymol. 54*, 411–435.

Dutton, P. L. (1986) *Encycl. Plant Physiol. 19*, 197–237.

Dutton, P. L., & Prince, R. C. (1978) in *The Photosynthetic Bacteria* (Clayton, R. K., & Sistrom, W. R., Eds.) Chapter 28, Plenum, New York.

Dutton, P. L., Petty, K. M., Bonner, H. S., & Morse, S. D. (1975) *Biochim. Biophys. Acta 387*, 536–556.

Errede, B., & Kamen, M. D. (1978) *Biochemistry 17*, 1015–1025.
Errede, B., Haight, G. P., & Kamen, M. D. (1976) *Proc. Natl. Acad. Sci. U.S.A. 73*, 113.
Feher, G., & Okamura, M. Y. (1978) in *The Photosynthetic Bacteria* (Clayton, R. K., & Sistrom, W. R., Eds.) Chapter 198, Plenum, New York.
Ferguson-Miller, S., Brautigan, D. L., & Margoliash, E. (1976) *J. Biol. Chem. 251*, 1104–1115.
Ferguson-Miller, S., Brautigan, D. L., & Margoliash, E. (1978) *J. Biol. Chem. 253*, 149–159.
Ferguson-Miller, S., Hochman, J., & Schindler, M. (1986) *Biochem. Soc. Trans. 14*, 822–824.
Hatefi, Y., & Stiggal, D. L. (1978) *Methods Enzymol. 53*, 5–10.
Hochman, J., Ferguson-Miller, S., & Schindler, M. (1985) *Biochemistry 24*, 2509–2516.
Ke, B., Chaney, T. H., & Reed, D. W. (1970) *Biochim. Biophys. Acta 216*, 373–383.
Konig, B. W., Osherhoff, N., Wilms, J., Muijsers, A. O., Dekker, H. L., & Margoliash, E. (1980) *FEBS Lett. 111*, 395–398.
Koppenol, W. H., & Margoliash, E. (1982) *J. Biol. Chem. 257*, 4426–4437.
Koppenol, W. H., Vroonland, C. A. J., & Braams, R. (1979) *Biochim. Biophys. Acta 503*, 499–508.
Malmstrom, B. G., & Andreasson, L. (1985) *J. Inorg. Biochem. 23*, 233–242.
Margoliash, E. (1979) *Proc. Natl. Acad. Sci. U.S.A. 76*, 155–159.
Margoliash, E., & Listgarten, J. (1962) *J. Biol. Chem. 237*, 3397–3405.
Margoliash, E., & Bosshard, H. R. (1983) *Trends Biochem. Sci. (Pers. Ed.) 8*, 316–320.
Meinhardt, S. W., & Crofts, A. R. (1982) *FEBS Lett. 149*, 223–227.
Minnaert, K. (1961) *Biochim. Biophys. Acta 50*, 23–34.
Moser, C. C., Giangiacomo, K. M., Matsuura, K., DeVries, S., & Dutton, P. L. (1986) *Methods Enzymol. 126*, 293–305.
Nicholls, P. (1965) in *Oxidases and Related Redox Systems* (King, T. E., et al., Eds.) pp 764–777, Wiley, New York.
Northrup, S. H., Reynolds, J. C. L., Miller, C. M., Forrest, K. F., & Boles, J. O. (1986) *J. Am. Chem. Soc. 108*, 8162–8170.
Overfield, R. E., & Wraight, C. A. (1980a) *Biochemistry 19*, 3322–3327.
Overfield, R. E., & Wraight, C. A. (1980b) *Biochemistry 19*, 3328–3334.
Overfield, R. E., & Wraight, C. A. (1986) *Photosynth. Res. 9*, 167–179.
Overfield, R. E., Wraight, C. A., & Devault, D. (1979) *FEBS Lett. 105*, 137–142.
Pachence, J. M., Dutton, P. L., & Blasie, J. K. (1978) *Biophys. J. 18*, 9a.
Pachence, J. M., Moser, C. C., Blasie, J. K., & Dutton, P. L. (1979a) *Biophys. J. 22*, 55a.
Pachence, J. M., Dutton, P. L., & Blasie, J. K. (1979b) *Biochim. Biophys. Acta 549*, 348–373.
Packham, N. K., Mueller, P., & Dutton, P. L. (1988) *Biochim. Biophys. Acta 933*, 70–84.
Prince, R. C., Cogdell, R. J., & Crofts, A. R. (1974) *Biochim. Biophys. Acta 347*, 1–13.
Reider, R., & Bosshard, H. R. (1980) *J. Biol. Chem. 255*, 4732–4739.
Rickle, G. K., & Cusanovich, M. A. (1979) *Arch. Biochem. Biophys. 197*, 589–598.
Rivas, E., Reiss-Husson, F., & le Maire, M. (1980) *Biochemistry 19*, 2943–2950.
Rosen, D., Okamura, M. Y., & Feher, G. (1979) *Biophys. J. 24*, 204a.
Rosen, D., Okamura, M. Y., & Feher, G. (1980) *Biochemistry 19*, 5687–5692.
Rosen, D., Okamura, M. Y., Albresch, E. C., Valkivs, G. E., & Feher, G. (1983) *Biochemistry 22*, 335–341.
Sinjorgo, K. M. C., Meijling, J. H., & Muijsers, A. O. (1984) *Biochim. Biophys. Acta 767*, 44–51.
Sinjorgo, K. M. C., Steinebach, O. M., Dekker, H. L., & Muijsers, A. O. (1986) *Biochim. Biophys. Acta 850*, 108–115.
Smith, M. B., Stonehuerner, H., Ahmed, A. J., Staudenmayer, N., & Millett, F. (1980) *Biochim. Biophys. Acta 592*, 303–313.
Speck, S. H., & Margoliash, E. (1984) *J. Biol. Chem. 259*, 1064–1072.
Speck, S. H., Ferguson-Miller, S., Osherhoff, N., & Margoliash, E. (1979) *Proc. Natl. Acad. Sci. U.S.A. 76*, 155–159.
Speck, S. H., Dye, D., & Margoliash, E. (1984) *Proc. Natl. Acad. Sci. U.S.A. 81*, 347–351.
Theorell, H., & Akesson, A. (1941) *J. Am. Chem. Soc. 63*, 1804–1811.
Tiede, D. M. (1985) *Biophys. J. 47*, 2a.
Tiede, D. M. (1987) *Biochemistry 26*, 397–410.
Vanderkooi, J., & Erecinska, M. (1974) *Arch. Biochem. Biophys. 162*, 385–391.
Vanderkooi, J. M., Maniara, G., & Erecinska, M. (1985) *J. Cell Biol. 100*, 435–441.
Von Smoluchowski, M. (1917) *Z. Phys. Chem. (Leipzig) 92*, 129–168.
Weber, P. C., & Tollin, G. (1985) *J. Biol. Chem. 260*, 5568–5573.
Weston, R. E., Jr., & Schwarz, H. A. (1972) *Chemical Kinetics*, Prentice-Hall, Englewood Cliffs, NJ.
Wilson, M. T., Greenwood, C., Brunori, M., & Antonini, E. (1975) *Biochem. J. 147*, 145–153.
Yonetani, T. (1967) *Method Enzymol. 10*, 332–335.